

Article

A Comprehensive Empirical Correlation for Finned Heat Exchangers with Parallel Plates Working in Oscillating Flow

Jiale Huang ^{1,2}, Mianli Liu ^{1,2} and Tao Jin ^{1,2,*}

¹ Institute of Refrigeration and Cryogenics, Zhejiang University, Hangzhou 310027, China; huangjiale@zju.edu.cn (J.H.); dallylau@zju.edu.cn (M.L.)

² Key Laboratory of Refrigeration and Cryogenic Technology of Zhejiang Province, Hangzhou 310027, China

* Correspondence: jintao@zju.edu.cn; Tel.: +86-571-8795-3233

Academic Editor: Artur J. Jaworski

Received: 20 November 2016; Accepted: 13 January 2017; Published: 8 February 2017

Abstract: The oscillating-flow heat transfer performance in finned heat exchangers is one of the main factors affecting the working efficiency of regenerative heat engines and refrigerators. In addition to the working parameters, the geometrical parameters of finned heat exchangers are also major influencing factors. In the present study, the ratio of the heat exchanger length and hydraulic diameter is applied as an independent similarity criterion. An experimental study has been carried out with six different geometrical dimensions of finned heat exchangers with parallel plates, in order to analyze the impacts of fin length, plate spacing, and corresponding relative fluid displacement amplitude, under various working conditions. Based on 298 tested points, a comprehensive empirical correlation for the finned heat exchangers with parallel plates working in oscillating flow has been proposed, providing a relatively accurate prediction, with 98.6% of data in the $\pm 20\%$ deviation and 83.9% of data in the $\pm 10\%$ deviation, within the range discussed.

Keywords: oscillating flow; heat transfer; finned heat exchanger; empirical correlation

1. Introduction

Regenerative thermal engines have various advantages, such as high efficiency, low noise production, and small vibrations, which enable wide application prospects in power engineering and energy utilization. One of the crucial components of a regenerative thermal engine is the heat exchanger working in oscillating flow [1]. The heat transfer performance of the heat exchanger directly determines the efficiency of the whole system. In order to improve the thermal efficiency of the oscillating-flow heat exchanger, it is necessary to study the dynamic heat transfer characteristics and the factors influencing the gas flow in heat exchangers. The optimization of the geometrical structure and working parameters of the oscillating-flow heat exchangers, can provide theoretical guidance for the design of highly efficient regenerative thermal engines.

According to the significant differences between the oscillating and steady flows, researchers have proposed a variety of methods for characterizing the heat transfer of an oscillating-flow heat exchanger. In 1967, Richardson [2] proposed an experimental correlation of steady-state flow in a cycle, in order to approximate the characterization of oscillating flow heat transfer, which is called the time-averaged steady flow equivalent (TASFE) model. Based on thermoacoustic theory, Nika et al. [3] mathematically developed the Nusselt number characterization method in the complex field. In 1986, Gedeon [4] was the first to verify the rationality of using averaged parameters of space and cycle in the momentum and energy equations. This method doesn't require an accurate measurement of the phase difference between the heat transfer temperature gap and the heat flow. In 1996, Zhao and Cheng [5] studied

the heat transfer characteristics of oscillating gas in a circular copper tube heated by constant heat flux. The average Nusselt number was correlated with the dimensionless amplitude and frequency, obtaining a preliminary empirical correlation. In 2007, Nsofor et al. [6] carried out a study on the heat transfer characteristics of the oscillating-flow heat exchanger, measuring the heat transfer in a finned-tube heat exchanger. Jaworski and Piccolo [7] obtained the temperature and velocity fields in a parallel plate channel heat exchanger, using the planar laser-induced fluorescence (PLIF) technique, combined with the particle image velocimetry (PIV). The relationship between the Nusselt number and the Reynolds number was thus obtained. Recently, Jaworski's group investigated the effect of fin length and fin spacing on the thermal performance of finned-tube heat exchangers [8]. The heat transfer rate can be predicted using the correlation between the heat transfer effectiveness, and the normalized fin spacing and fin length. In the past decade, researchers have been approaching a deeper understanding of the oscillating flow behaviors, using state-of-the-art techniques [9–14].

Tang et al. [15,16] experimentally studied the influence of working conditions, as well as the compression-expansion effect, on the Nusselt number of finned heat exchangers. An empirical correlation of the Nusselt number, with the maximum Reynolds number and Valensi number, has been summarized. Following the analysis and optimization method, this work aims to introduce the geometrical parameters as major factors of the heat transfer performance prediction. It presents an empirical correlation for the finned heat exchanger working in oscillating flow, which comprehensively considers velocity amplitude, oscillating frequency, pressure ratio, and geometrical dimension during the heat transfer process. In the following discussion, the dimensionless parameters are defined as:

$$Re_{\max} = \frac{u_A d_h}{\nu}, \quad (1)$$

$$Va = \frac{\omega d_h^2}{\nu}, \quad (2)$$

$$Nu = \frac{h d_h}{k}, \quad (3)$$

$$PR = \frac{p_{m1} + p_{A1}}{p_{m1} - p_{A1}}, \quad (4)$$

where u_A and ω are the velocity amplitude and angular frequency of the flow, respectively. h is the mean convective heat transfer coefficient. ν and k are the kinetic viscosity and thermal conductivity of the fluid, respectively. d_h is the hydraulic diameter.

For the cross-section shape of the flow channels in fin-type heat exchangers, the geometry primarily depends on the channel length l and hydraulic diameter d_h . In the design of heat exchangers working in oscillating flow, the length direction, parallel to the direction of oscillating fluid, is constrained by the gas peak-to-peak displacement. The transverse dimension, perpendicular to the direction of oscillating fluid, is limited by the thermal penetration depth δ_k , which is defined as:

$$\delta_k = \sqrt{\frac{2k}{\omega \rho_m c_p}}, \quad (5)$$

where ρ_m and c_p are the mean density and the isobaric specific heat of the fluid, respectively.

Swift [17] pointed out that the relative displacement amplitude has an important effect on the heat transfer performance. The relative displacement amplitude A_r is the ratio of the peak-to-peak displacement value and the channel length, which is defined as follows:

$$A_r = \frac{2x_A}{l} = \frac{2u_A}{\omega l}, \quad (6)$$

where x_A is the displacement amplitude of the flow. Hofler [18] and Piccolo [19] suggested that the A_r value should be close to, or larger than, one. In fact, A_r is not an independent geometrical parameter and can be practically transformed into an expression, including the dynamic parameters, as follows:

$$A_r = \left(\frac{2Re_{\max}}{Va} \right) / \left(\frac{l}{d_h} \right) \quad (7)$$

Equation (6) indicates that the influence of geometrical parameters on heat transfer performance can be discussed in relation to the controlled working conditions. As a geometrical parameter of the heat exchanger, l/d_h can be correlated as a major factor when considering the heat transfer characteristics.

Following the work presented in Reference [15], this paper presents an experimental study using six different geometrical dimensions of finned heat exchangers with parallel plates, in order to analyze the impacts of fin length, plate spacing, and corresponding relative fluid displacement amplitude, under various working conditions. This is completed in order to propose a comprehensive empirical correlation for the finned heat exchangers with parallel plates working in oscillating flow, displaying a wider range of application.

2. Experimental Methods

In order to simulate the actual working conditions of heat exchangers in regenerative thermal engines, an experimental setup is established to measure the heat transfer characteristics of the finned heat exchangers with oscillating flow conditions. The working fluid is helium. Figure 1 presents the schematic diagram of the experimental setup, and more details can be found in [15].

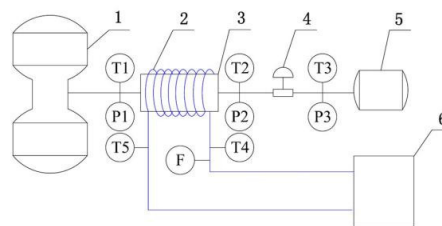


Figure 1. Schematic diagram of the experimental apparatus (1—Linear compressor; 2—Cooling water loop; 3—Testing section; 4—Adjusting valve; 5—Reservoir; 6—Thermostat).

A linear compressor (Manufactured by Lihan Thermoacoustic Technologies Co., Ltd., Shenzhen, China) is used to generate pressure wave in oscillating flow. The compressor is driven by variable-frequency power supplies so as to indirectly control the oscillating frequency of the flow by adjusting the frequency of the compressor. The input work of the compressor is controlled within 2.5 kW and the operating current is controlled below 11 A. A variable-frequency power supply allows the voltage and current limits to be set according to load characteristics required by programmable logic controllers. A frequency range of 0 Hz to 650 Hz, and a resolution of 0.01 Hz, are accessible. The combination of an adjusting valve and a gas reservoir structure is used to control and measure the velocity amplitude of the flow. More specifically, for oscillating flow, the adjusting valve and the gas reservoir can be analogous to resistance and capacity impedance, in series with the required values achieved by changing the valve opening, which controls the velocity amplitude into and out of the reservoir. By measuring the pressure wave in the gas reservoir, combined with the volume of the gas reservoir and the physical properties of the working fluid, the magnitude of the oscillating flow velocity amplitude can be determined. The heat exchanger, connected channels, and water pipes, are all thermally insulated by polystyrene foam in order to minimize the heat leakage to the surroundings.

Systematic experimental design is carried out and is based on the Box-Behnken Design (BBD), a standard method of response surface methodology (RSM) [20]. RSM is a method used to optimize the

experimental conditions, suitable for solving nonlinear data processing-related problems, including techniques such as experimental design, modeling, testing the suitability of the model, searching for the best combination of conditions, and so on. Through the process of regression fitting and contour drawing, the corresponding response value of each factor's level can be easily identified. Based on the response values, the optimal response values and the corresponding experimental conditions can be obtained. At the same time, RSM can also be used to fit complex unknown function relations in a small area, with a simple first or second order polynomial model. The relatively simple calculation reduces the development cost and improves the product quality for solving the practical problems in data processing. The software Design-Expert (Version 8.0.6, Stat-Ease Inc., Minneapolis, MN, USA) is applied in order to choose the maximum Reynolds number, the Valensi number, and l/d_h as the first-level influencing factors. After setting the corresponding names, units, and ranges, experimental operating points are suggested as a guidance for obtaining the correct experimental results, and are listed in a table with 18 typical testing points. It is proposed that these are carried out first for a quicker and better identification of each parameter's influence and trend of optimal results. In the experiments designed by RSM, the mean pressure was fixed at 3 MPa and the pressure ratio was fixed at 1.2. The maximum Reynolds number ranged from 400 to 1200 (velocity amplitude ranged from 1.0 m/s to 3.8 m/s, correspondingly), and the Valensi number ranged from 150 to 250 (working frequency ranged from 40 Hz to 90 Hz, correspondingly). With a clear understanding of each parameter's impact on the Nusselt number, indicated by the response surface, the working ranges of the system were extended to include Re_{\max} values between 200 and 1200, Va values between 100 and 350, and a pressure ratio between 1.1 and 1.3.

The heat exchangers with parallel-plate channels exhibiting various l/d_h values are numbered and listed in Table 1, where Case A represents $d_h = 1.5$ mm and Case B represents $d_h = 1.8$ mm. For Case A and Case B with the same hydraulic diameter, the heat exchanger number is followed by 1, 2, or 3, to indicate a length of 15 mm, 20 mm, and 30 mm, respectively. Figure 2 shows the illustration and photo of a typical parallel-plate heat exchanger (Case A1).

Table 1. Geometrical parameters of the tested heat exchangers.

Heat Exchanger Number	l (mm)	d_h (mm)	l/d_h	Heat Exchanger Number	l (mm)	d_h (mm)	l/d_h
A1	15	1.5	10	B1	15	1.8	8.3
A2	20	1.5	13.3	B2	20	1.8	11.1
A3	30	1.5	20	B3	30	1.8	16.7

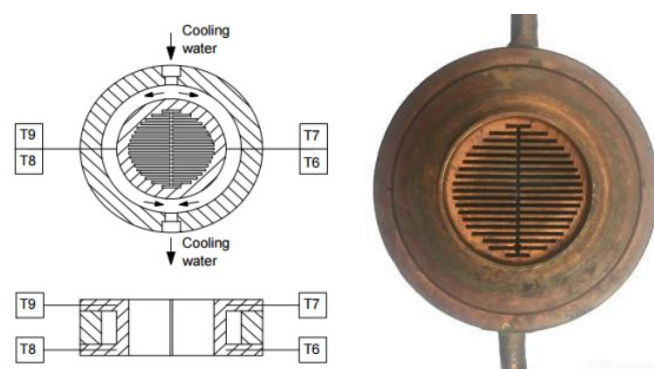


Figure 2. Illustration and photo of a typical tested heat exchanger (A1: $l = 15$ mm, $d_h = 1.5$ mm, $l/d_h = 10$).

Due to the heat leakage to the surroundings, the coefficient ξ is introduced into the calculation of the heat transfer rate Q_h of the gas side in the flow channel. The coefficient ξ is defined as the ratio of the actual heat transfer rate Q_h and the cooling water heat transfer rate Q_c . Q_c can be calculated as:

$$Q_c = q_v \rho_{\text{water}} c_{\text{water}} (t_2 - t_1) \quad (8)$$

where q_v is the cooling water flow rate, and ρ_{water} and c_{water} are the density and heat capacity of water, respectively. t_1 and t_2 are the inlet and outlet temperatures of the cooling water, respectively. Because of the use of the same thermal insulation method as in Ref. [15], the expression of coefficient ξ is taken as:

$$\xi = \frac{Q_h}{Q_c} = \frac{1}{1 - (Q_h - Q_c)/Q_h} = \frac{1}{1 + 5.43 \times 10^{-5} t_h^2 - 3.556 \times 10^{-2} t_h + 5.77} \quad (9)$$

where t_h is the average temperature of the cooling water.

3. Measurement Uncertainty

The experimental results are finally characterized as the average Nusselt number, which is actually a function of nine measured parameters. The Nusselt number is calculated using the following expression:

$$Nu = \frac{h d_h}{k} = \frac{\xi Q_c d_h}{k A_s (t_f - t_{wi})} = \frac{\xi d_h c_{\text{water}} \rho_{\text{water}} (t_2 - t_1) q_v}{k A_s (t_f - t_{wi})} \quad (10)$$

where A_s is the calculated effective heat transfer area for each finned heat exchanger; t_f and t_{wi} are the mean temperatures of the fluid and wall on the internal side, respectively.

Since the measurement errors of different variables are independent of each other, according to the principle of error propagation, the uncertainty of the Nusselt number is:

$$\sigma_{Nu} = \sqrt{\sum_{i=1}^9 \left(\frac{\partial f}{\partial x_i} \right)^2 \sigma_{x_i}^2} \quad (11)$$

where $\partial f / \partial x_i$ is the partial derivative of the function on one of the measured parameters. σ_{x_i} is the uncertainty of each measured parameter. For simplicity, the influence of five measurement errors on the Nusselt number were considered, including the inlet and outlet cooling water temperatures t_1 and t_2 , the fluid mean temperature t_f , the mean wall temperature t_{wo} on the external side, and the cooling water flow rate q_v . According to the principle of error propagation:

$$\begin{aligned} \left(\frac{\partial f}{\partial x_i} \right)^2 &= \left(\frac{\partial Nu}{\partial q_v} \right)^2 = \left(\frac{\xi d_h c_{\text{water}} (t_2 - t_1)}{k A_s (t_f - t_{wo})} \right)^2 \\ \left(\frac{\partial f}{\partial x_i} \right)^2 &= \left(\frac{\partial Nu}{\partial q_v} \right)^2 = \left(\frac{\xi d_h c_{\text{water}} (t_2 - t_1)}{k A_s (t_f - t_{wo})} \right)^2 \\ \left(\frac{\partial f}{\partial x_i} \right)^2 &= \left(\frac{\partial Nu}{\partial t_f} \right)^2 = \left(\frac{\partial Nu}{\partial t_{wo}} \right)^2 = \left(\frac{\xi d_h c_{\text{water}} q_v (t_2 - t_1)}{k A_s (t_f - t_{wo})^2} \right)^2 \end{aligned} \quad (12)$$

After calculating the error propagation, the total uncertainty of the Nusselt number can be obtained, according to Equation (10).

4. Results and Discussion

Firstly, in order to produce a quick sketch of self-consistency and the impact trends of parameters, the analysis of variance is carried out to show the normal distribution plot of the residuals of 18 typical tested points (shown in Figure 3), which indicates self-consistency of the results. In Figure 3, the data show the normal probability distribution of residuals after an analysis of variance (ANOVA) of the tested results. The horizontal axis stands for the internally studentized residual, which is the quotient resulting from the division of a residual by an estimate of its standard deviation. The vertical axis stands for its corresponding normal possibility, which has exponential coordinates, hence, the

normal distribution plot of residuals can show its self-consistency if the data lie in a neat straight line. The maximum deviation is below 10% with the correlation fitting based on RSM. The three-dimensional response surface is plotted into a polynomial correlation, with the highest order of two. Figure 4 shows the response surface plot with a fixed maximum Reynolds number of 800 for demonstration.

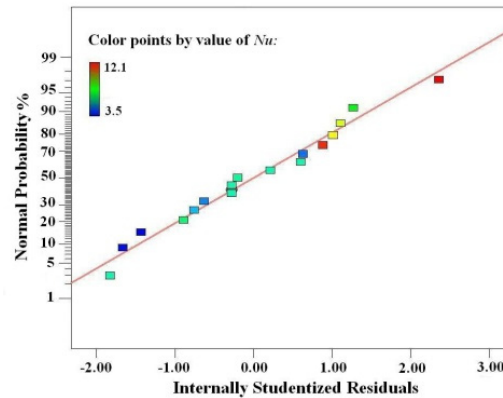


Figure 3. Normal plot of residuals for 18 typical tested points.

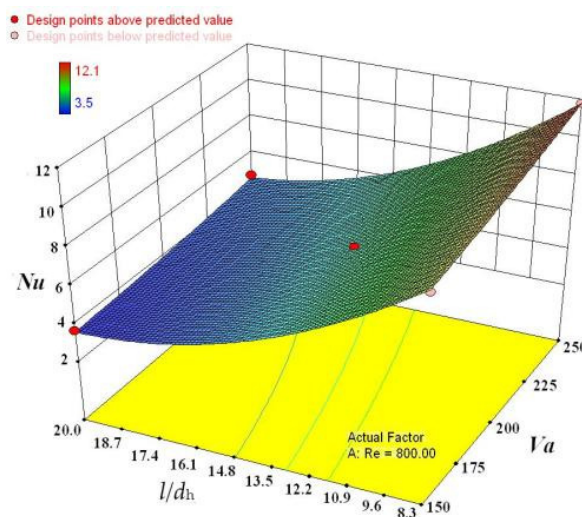


Figure 4. Response surface with a fixed maximum Reynolds number of 800.

From the response surfaces with fixed various parameters, it is noted that l/d_h , as a geometrical parameter, has a negative influence on the Nusselt number. The rise of l/d_h leads to a dramatic weakening in the heat transfer performance. Along with the fact that the maximum Reynolds number and Valensi number both have a positive impact on the Nusselt number, more detailed experimental results are obtained with error bars indicating the uncertainty of acquired data, which is not higher than 5.8%.

Figures 5–7 present the Nusselt number variations with six different l/d_h values when the Valensi numbers are 150, 200, and 250, respectively. These values are realized by the combination of three different lengths and two different hydraulic diameters, as listed in Table 1. It can be seen from the figures that, when the Reynolds number and Valensi number are both a controlled constant, the Nusselt number decreases as l/d_h is increased, reflected in the response surface illustrated in Figure 4. The oscillating-flow heat transfer performance will be significantly weakened when l/d_h is increased within the range discussed.

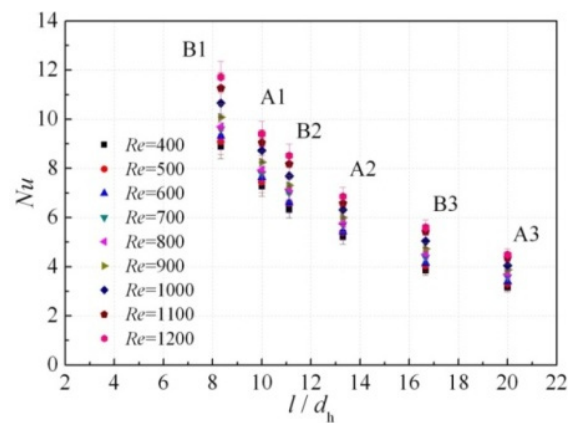


Figure 5. Nusselt number variation with l/d_h , $Va = 150$.

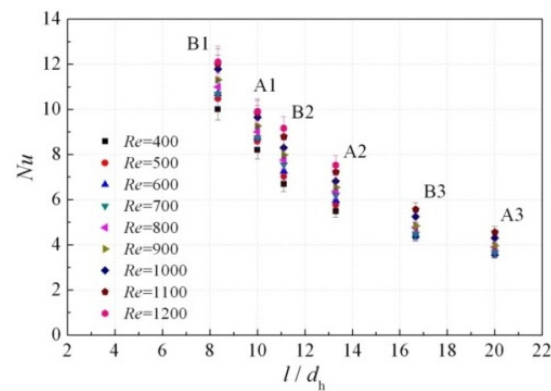


Figure 6. Nusselt number variation with l/d_h , $Va = 200$.

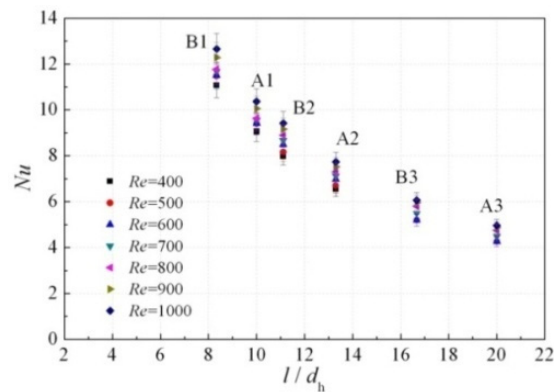


Figure 7. Nusselt number variation with l/d_h , $Va = 250$.

The results indicate that when the hydraulic diameter of the channel (roughly twice of the plate spacing) is constant, for the heat transfer with a smaller length (l/d_h is relatively small), the heat transfer performance of the parallel plates in oscillating helium flow is significantly better than that of heat exchangers with longer fins. It is assumed that the heat transfer process is enhanced by the entrance effect of oscillating flow. In addition, if the heat exchanger length is too large, being even longer than the peak-to-peak displacement of working fluid, part of the fluid particles will be trapped in the flow channel experiencing the reciprocating motion. As the “trapped” fluid has a temperature similar to that of the wall, the oscillating heat transfer will be relatively weak. From the view of the whole heat exchanger, it can be regarded that the central part of the heat transfer area doesn’t play

a good role in the heat transfer process, which will lead to a lower Nusselt number of the oscillating flow inside the entire channel. With longer channels, there will be a larger area that has no effective heat transfer. Hence, for the heat exchanger types A and B, the obtained magnitudes have orders of $B1 > B2 > B3$ and $A1 > A2 > A3$. Numerical simulation by Ishikawa et al. [21] showed that the net heat transfer rate between solid and fluid states mainly occurred on the inlet and outlet faces of the heat exchanger with parallel plates. When the fin length is increased, the heat flux on inlet and outlet faces can be positive or negative, leading to a decrease in the net heat flux. As a result, it is also possible that the heat transfer performance of the oscillating flow in the heat exchanger with a length of 15 mm, is much better than the others due to the increased heat transfer rate per unit area.

Figures 8–10 present the Nusselt number variations of Ar when Valensi numbers are 150, 200, and 250, respectively. These figures also show that for heat exchangers with the same hydraulic diameter, but different length, the Nusselt number decreases as the heat exchanger length is increased. It can be seen that when Re and Va are controlled, heat exchangers with a length of 20 mm (A2 and B2) have about a 30% lower Nu number than those with a length of 15 mm (A1 and B1), and heat exchangers with a length of 30 mm (A3 and B3) have about a 50% lower Nu number than those with a length of 15 mm. When considering those with a length of 15 mm (A1 and B1), it is evident that better heat transfer performance mainly occurs when Ar is larger than 1, supporting the conclusion offered by Hofler [18] and Piccolo [19]. In fact, when Re and Va are controlled constants, the relative fluid displacement amplitude Ar is equivalent to the reciprocal of l/d_h .

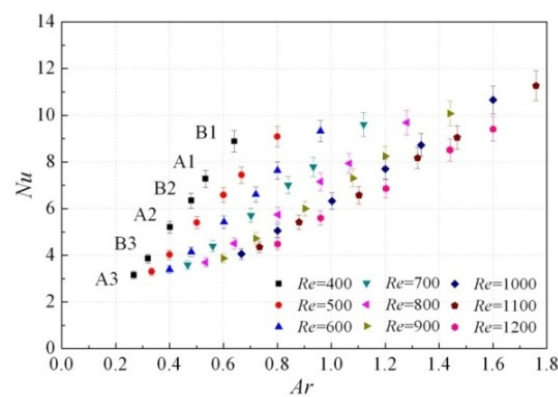


Figure 8. Nusselt number variation with Ar , $Va = 150$.

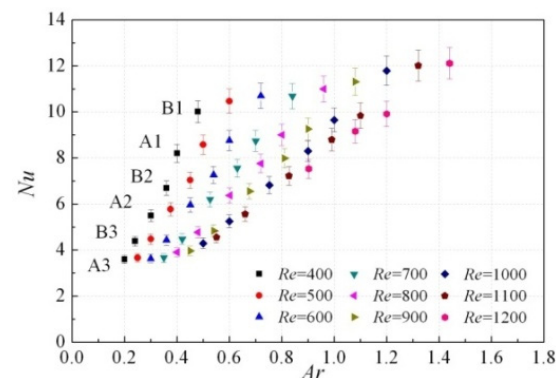


Figure 9. Nusselt number variation with Ar , $Va = 200$.

Compared to Figures 5–7, the Nu variations of Ar reflect the same physical pattern. However, the impact of relative fluid displacement amplitude is actually a result of comprehensive effects; an aspect which has been neglected in the previous study. Piccolo [22] numerically studied the relationship between the mean convective heat transfer coefficient h , and the relative displacement amplitude

A_r , under the same pressure ratio based on energy conservation. Results showed that remarkably, h increased with increasing A_r when $A_r > 1$, while h remained constant when $A_r \leq 1$, which does not reflect the results concluded in this paper. As A_r includes the geometrical parameters, as well as the impacts of Re and Va , it is difficult to explain the direct relationship between the oscillating-flow heat transfer and each parameter. In comparison, l/d_h , instead of A_r , can be chosen as an important geometrical parameter, which should be taken into account when considering the empirical correlation for the finned heat exchangers with parallel plates, working under oscillating conditions.

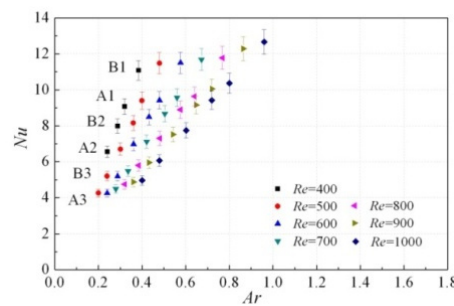


Figure 10. Nusselt number variation with A_r , $Va = 250$.

Figures 11–13 present the actual heat transfer rate variations of A_r when the Valensi numbers are 150, 200, and 250, respectively. The results show that, for the same type of heat exchanger with the same hydraulic diameter, there exists an optimal fin length for achieving the required heat load. Out of the three lengths tested, the length of 20 mm achieves the largest heat transfer rate for each working condition. In the practical design of regenerative thermal systems, the fin efficiency and the effective heat transfer area should be considered, as well as the space-cycle average Nusselt number.

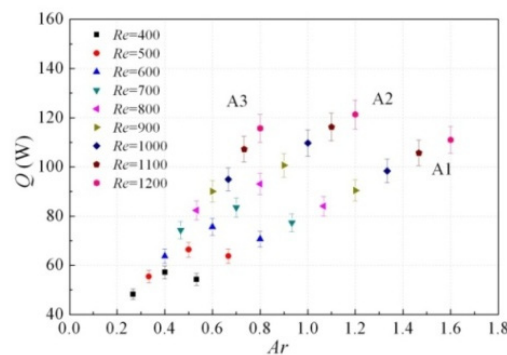


Figure 11. Heat transfer rate variation with A_r , $Va = 150$.

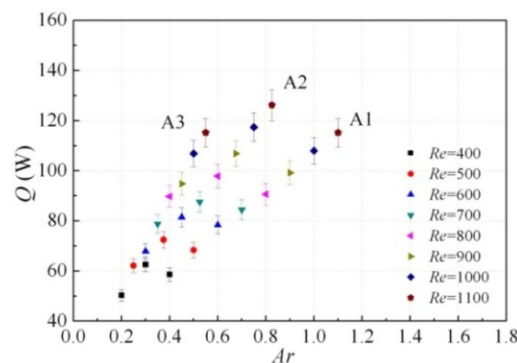


Figure 12. Heat transfer rate variation with A_r , $Va = 200$.

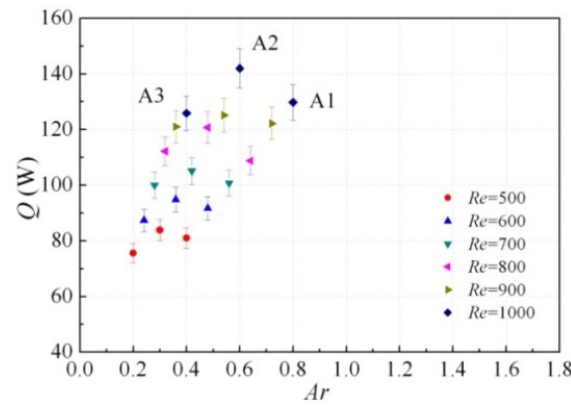


Figure 13. Heat transfer rate variation with Ar , $Va = 250$.

In order that the experimental data can be conveniently applied to the design of finned heat exchangers working under oscillating conditions in regenerative thermal engines, further data fitting was implemented to obtain a relatively comprehensive empirical correlation. The Reynolds number, Valensi number, Mach number, Prandtl number, specific heat ratio, ratio of length and hydraulic diameter, and pressure ratio PR , are considered as the main similarity criteria relating to the oscillating-flow heat transfer in heat exchanging channels [5]. This experiment adopted helium gas as the working fluid, so the specific heat ratio and Prandtl number can be considered as nearly constant. In addition, the Mach number implies the compressibility of fluid, which was kept at a value much lower than one in the experiment. Finally, based on the discussion above, the expression of the empirical correlation is defined as:

$$Nu = aPR^b \left(\frac{l}{d_h} \right)^c Re^m Va^n \quad (13)$$

It is ascertained that $b = 6.138$ from the linear fitting of $\log(Nu)$ and $\log(PR)$ with a coefficient determination of $R^2 = 0.9798$, as shown in Figure 14. Following this, $\log(Nu/PR^{6.138})$ and $\log(Re_{\max})$ are linearly fitted with a slope of $m = 0.153$ and a coefficient determination of $R^2 = 0.8158$. Next, by completing $\log(Nu/PR^{6.138}/Re_{\max}^{0.153})$ and $\log(Va)$ linear fitting with $n = 0.504$ and $R^2 = 0.8296$, the coefficient c is determined as -1.137 and a is calculated from the intercept, producing a value of 1.021. Figures 14–17 show the determination of all the coefficients.

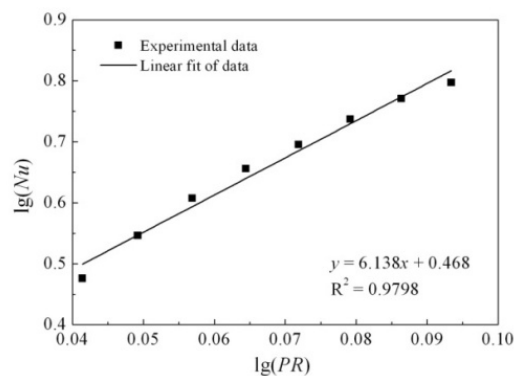
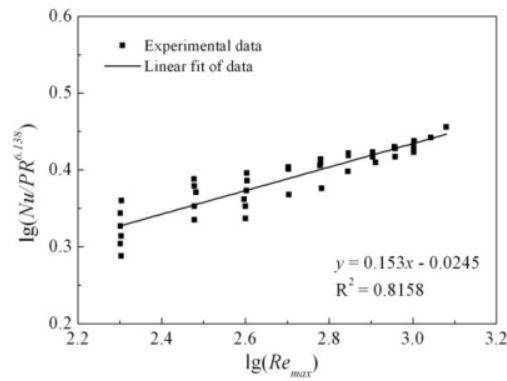
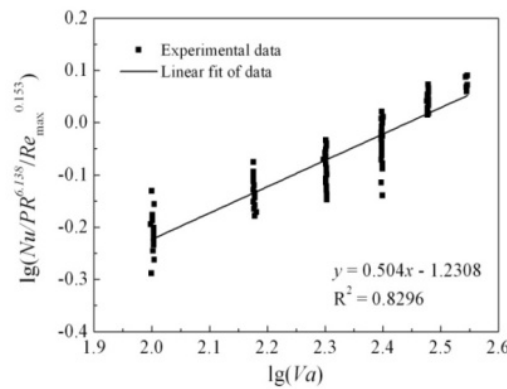
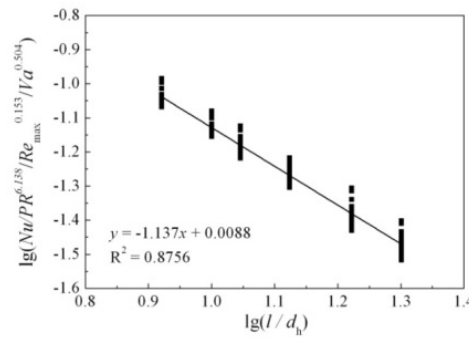


Figure 14. Determination of coefficient b .

Figure 15. Determination of coefficient m .Figure 16. Determination of coefficient n .Figure 17. Determination of coefficients c and a .

As a result, within the ranges used in the experiments, i.e., $200 < Re_{\max} < 1200$, $100 < Va < 350$, $1.1 < PR < 1.3$, and $8.3 < l/d_h < 20$, the space-cycle average Nusselt number of oscillating-flow heat transfer in the finned heat exchanger with parallel plates, can be predicted using the following correlation:

$$Nu = 1.021 \frac{PR^{6.138} Re^{0.153} Va^{0.504}}{(l/d_h)^{1.137}} \quad (14)$$

To prove the self-consistency of the empirical correlation, the predicted results are compared to the corresponding experimental results, as shown in Figure 18. Out of the total 298 tested data points, 98.6% of the predicted points lie within a deviation of $\pm 20\%$, and 83.9% of the predicted points lie within a deviation of $\pm 10\%$, indicating that the comprehensive empirical correlation is able to provide acritical guidance for the design of finned heat exchangers in regenerative thermal engines.

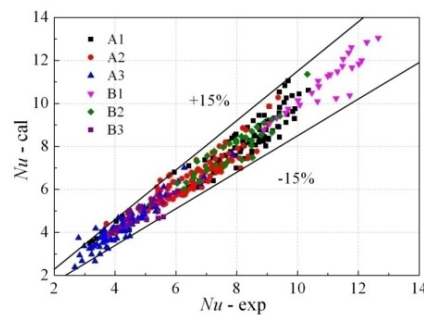


Figure 18. Comparison of calculated data with experimental data.

5. Conclusions

The space-cycle average Nusselt number is introduced to characterize the heat transfer performance of oscillating helium flow in the finned heat exchangers with parallel plates. The relationship between the Nusselt number and l/d_h , and the relative fluid displacement amplitude A_r , are analyzed based on experimental results, respectively. A decrease in l/d_h leads to a remarkable increase in the Nusselt number. Therefore, l/d_h appears to be the most appropriate choice in terms of the actual value of the heat transfer rate. An A_r value which is larger than one improves the oscillating-flow heat transfer inside the parallel plates. It is suggested that l/d_h would be a more reasonable parameter for characterizing the geometrical similarity. Based on a total number of 298 tested points, a comprehensive empirical correlation for finned heat exchangers with parallel plates working in oscillating flow, has been proposed. A total of 98.6% of the predicted points lie within a deviation of $\pm 20\%$, and 83.9% of the predicted points lie within a deviation of $\pm 10\%$, which indicates that the comprehensive empirical correlation is able to provide critical guidance for the design of finned heat exchangers in regenerative thermal engines.

Acknowledgments: The project is financially supported by the National Key Basic Research Program of China (No. 613322) and the National Natural Science Foundation of China (No. 51576170).

Author Contributions: Jiale Huang and Tao Jin conceived and designed the experiments; Mianli Liu performed the experiments; Jiale Huang and Mianli Liu analyzed the data; Tao Jin contributed analysis tools; Jiale Huang and Tao Jin wrote the paper.

Conflicts of Interest: The authors declare no conflict of interest.

References

1. Jin, T.; Huang, J.L.; Feng, Y.; Yang, R.; Tang, K.; Radebaugh, R. Thermoacoustic prime movers and refrigerators: Thermally powered engines without moving components. *Energy* **2015**, *93*, 828–853. [\[CrossRef\]](#)
2. Richardson, P.D. Effects of sound and vibration on heat transfer. *Appl. Mech. Rev.* **1967**, *20*, 201–217.
3. Nika, P.; Bailly, Y.; Guermeur, F. Thermoacoustics and related oscillatory heat and fluid flows in micro heat exchangers. *Int. J. Heat Mass Transf.* **2005**, *18*, 3773–3792. [\[CrossRef\]](#)
4. Gedeon, D. Mean-parameter modeling of oscillating flow. *J. Heat Transf.* **1986**, *108*, 513–518. [\[CrossRef\]](#)
5. Zhao, T.S.; Cheng, P. Oscillatory heat transfer in pipe subjected to a laminar reciprocating flow. *J. Heat Transf.* **1996**, *3*, 92–597. [\[CrossRef\]](#)
6. Nsofor, E.C.; Celik, S.; Wang, X.D. Experimental study on the heat transfer at the heat exchanger of the thermoacoustic refrigerating system. *Appl. Therm. Eng.* **2007**, *27*, 2435–2442. [\[CrossRef\]](#)
7. Jaworski, A.J.; Piccolo, A. Heat transfer processes in parallel-plate heat exchangers of thermoacoustic devices—Numerical and experimental approaches. *Appl. Therm. Eng.* **2012**, *42*, 145–153. [\[CrossRef\]](#)
8. Kamsanam, W.; Mao, X.N.; Jaworski, A.J. Thermal performance of finned-tube thermoacoustic heat exchangers in oscillatory flow conditions. *Int. J. Therm. Sci.* **2016**, *101*, 169–180. [\[CrossRef\]](#)
9. Jaworski, A.J.; Mao, X.N.; Mao, X.R.; Yu, Z.B. Entrance effects in the channels of the parallel plate stack in oscillatory flow conditions. *Exp. Therm. Fluid Sci.* **2009**, *33*, 495–502. [\[CrossRef\]](#)

10. Yu, Z.B.; Mao, X.N.; Jaworski, A.J. Experimental study of heat transfer in oscillatory gas flow inside a parallel-plate channel with imposed axial temperature gradient. *Int. J. Heat Mass Transf.* **2014**, *77*, 1023–1032. [[CrossRef](#)]
11. Kamsanam, W.; Mao, X.N.; Jaworski, A.J. Development of experimental techniques for measurement of heat transfer rates in heat exchangers in oscillatory flows. *Exp. Therm. Fluid Sci.* **2015**, *62*, 202–215. [[CrossRef](#)]
12. Mathie, R.; Markides, C.N. Heat transfer augmentation in unsteady conjugate thermal system—Part I: Semi-analytical 1-D framework. *Int. J. Heat Mass Transf.* **2013**, *1*, 802–818. [[CrossRef](#)]
13. Mathie, R.; Nakamura, H.; Markides, C.N. Heat transfer augmentation in unsteady conjugate thermal systems-Part II: Applications. *Int. J. Heat Mass Transf.* **2013**, *1*, 819–833. [[CrossRef](#)]
14. Mathie, R.; Markides, C.N.; White, A.J. A framework for the analysis of thermal losses in reciprocating compressors and expanders. *Heat Trans. Eng.* **2014**, *16–17*, 1435–1449. [[CrossRef](#)]
15. Tang, K.; Yu, J.; Jin, T.; Wang, Y.P.; Tang, W.T.; Gan, Z.H. Heat transfer of laminar oscillating flow in finned heat exchanger of pulse tube refrigerator. *Int. J. Heat Mass Transf.* **2014**, *70*, 811–818. [[CrossRef](#)]
16. Tang, K.; Yu, J.; Jin, T.; Gan, Z.H. Influence of compression-expansion effect on oscillating-flow heat transfer in a finned heat exchanger. *J. Zhejiang Univ. Sci. A* **2013**, *14*, 427–434. [[CrossRef](#)]
17. Swift, G.W. Thermoacoustic engines. *J. Acoust. Soc. Am.* **1988**, *84*, 1145–1180. [[CrossRef](#)]
18. Hofler, T.J. Effective heat transfer between a thermoacoustic heat exchanger and stack. *J. Acoust. Soc. Am.* **1993**, *94*, 1772. [[CrossRef](#)]
19. Piccolo, A. Numerical computation for parallel plate thermoacoustic heat exchangers in standing wave oscillatory flow. *Int. J. Heat Mass Transf.* **2011**, *54*, 4518–4530. [[CrossRef](#)]
20. Chiang, K.T. Modeling and optimization of designing parameters for a parallel-plain fin heat sink with confined impinging jet using the response surface methodology. *Appl. Therm. Eng.* **2007**, *27*, 2473–2482. [[CrossRef](#)]
21. Ishikawa, H.; Mee, D.J. Numerical investigation of flow and energy fields near a thermoacoustic couple. *J. Acoust. Soc. Am.* **2002**, *111*, 831–839. [[CrossRef](#)] [[PubMed](#)]
22. Piccolo, A.; Pistone, G. Estimation of heat transfer coefficients in oscillating flow: The thermoacoustic case. *Int. J. Heat Mass Transf.* **2006**, *49*, 1631–1642. [[CrossRef](#)]



© 2017 by the authors; licensee MDPI, Basel, Switzerland. This article is an open access article distributed under the terms and conditions of the Creative Commons Attribution (CC BY) license (<http://creativecommons.org/licenses/by/4.0/>).